Estimation of the ROV hydrodynamic coefficients using CFD

Mohamed Ahmed Soliman
Department of Ships and Submarine, Military Technical College, Egypt, MohamedSoliman5899@gmail.com

Supervisor: Col. Dr. Mohamed Ibrahim Bennaya, Commandor. Dr. Mohamed Youssef
Department of Ships and Submarine, Military Technical College, Egypt, mbennaya@mtc.edu.eg, *mh.youssefharb@gmail.com*

Abstract– Dynamics model is essential and critical for the successful design of navigation and control system of an underwater vehicle. In this paper, the equation of motion of the ROV was estimated by using numerical methods. And this was done by using many software have been used such as SOLIDWORKS, ANSYS FLUENT, ANSYS CFX and COMSOL MULTIPHYSICS. The equation of motion in 6 DOF consists of mass and inertia parameters found by SOLIDWORKS. Damping parameters including linear and quadratic damping estimated using steady state simulation in ANSYS FLUENT. Another component in the equation of motion is the added mass parameter and this can be estimated by applying free undamped oscillation of ROV in water with a spring using Fluid structure interaction in COMSOL MULTIPHYSICS software. The results show that the CFD can provide the hydrodynamic property for the ROV as well. The thrust configuration matrix can be also estimated by measuring the distances from the thrusters to the center of gravity.

Keywords-- Damping parameters; Added Mass; Dynamic Model; Thrust configuration matrix.

I. INTRODUCTION (HEADING 1)

Under-water missions require a high quality Remotely Operated Vehicle (ROV) specially designed for operating in confined and precarious conditions that are found in ports. ROVs are easy robots for many difficult applications which human can't perform well in different environment conditions. ROV can clean the underwater hull body, take photos under the water, and move objects from one place to another.

ROV needs a high-quality performance PID controller for guidance and navigation control of the ROV and to control the thrust force of the thrusters in all degrees of freedom in addition to controlling its velocity under the water. The PID controller produces generalized control forces and the control allocation distributes these generalized control forces to the actuators [1].

To make a PID controller, the equation of motion of the ROV in all degrees of freedom must be estimated. To do this, some experimental tests must be performed to estimate the components of the equation of motion. The equation of motion is divided into three types of parameters, mass and inertia parameters, damping parameters, added mass parameters and thruster configuration.

Two main theories of maneuvering and seakeeping are often used to model the effect of external forces and moments on a marine craft. In maneuvering theory, the vessel is moving in calm water without wave excitation and the hydrodynamic coefficients are assumed to be frequency independent such that the nonlinear mass damper spring system contains constant hydrodynamic coefficients whereas wave excitation is acknowledged in seakeeping theory. Since underwater vehicles are considered to operate below the wave affected zone, they can be modeled with constant added mass and damping coefficients [2].

There have been a wide range of methodologies proposed to estimate the hydrodynamic coefficients of dynamic equations of motion for unmanned underwater vehicles. Conventional methods include tow tank experiments by using the underwater vehicle itself [3] or a scale model of it (Nomoto and Hattori 1986) while measuring the forces and moments applied to the vehicle under various operating circumstances. A routine dynamic testing of utilizing a Planar Motion Mechanism (PMM) above the towing tank was introduced [4] to shift the ROV in a planar motion. Since a PMM mounted in a towing tank can move the ROV in multiple directions by rotating the ROV, it allows a complete model identification of hydrodynamic coefficients in all 6 DOFs to be attained. However, PMMs are fairly costly and the test procedures consume significant amount of time.

The classical free decay test applied in determining hydrodynamic coefficients has been introduced by Morrison and Yoerger in which the ROV oscillated in the water using three springs and the parameters in a single DOF of heave motion were identified while the position data was measured by SHARPS [5].

The motion equations can be derived by using the Newton-Euler formulation on the basis of Newton's Second Law or using Euler-Lagrange equation in mechanics [6]. Newtonian and Lagrangian mechanics have been discussed in detail in literature extensively [7]. The physical properties of the system contain rigid-body and hydrodynamic models [8,10, and 11].

By using the robot model, the rigid-body kinetics in complete 6 DOFs can be derived and represented in a vectorial form.

A Numerical approach of Computational Fluid Dynamic (CFD), which solves the Navier-Stokes equations in fluid dynamics, has been used for hydrodynamic computations of underwater vehicles in recent years [9].

In this paper, mass and inertia terms were calculated using SOLIDWORKS, damping parameters were estimated using ANSYS CFX and ANSYS FLUENT, added mass parameters were estimated using COMSOL MULTIPHYSICS by simulation of free decay test under the water.

II. METHODOLOGY

Design parameters are explained and some assumptions were used:

1. The ROV is neutrally buoyant (the total density of ROV and the density of the surrounding fluid are equal) allowing the ROV to remain at a fixed position for a specified amount of time.
2. The center of volume (the point of application of buoyancy force) of the ROV is above the center of gravity and both are located on the same vertical line to provide stability to the ROV. A variation in roll or pitch angles is compensated by a restoring moment created by the weight and the buoyancy forces.
3. The ROV is made from Polypropylene material.

A. *Mechanical Design*

TABLE I
ROV MECHANICAL PARAMETERS

Property	Value
Net weight	14.6709 Kg
Volume	17088.40 cm^3
Length	757.5 mm
Width	556.3 mm
Height	370.9 mm
T-200 thruster	6.7 Kgf
Density of Polypropylene	908 Kg/m^3

B. *Dynamic Model*

The ROV equation of motion are written as:

$$\boldsymbol{M_{RB}}\dot{v} + \boldsymbol{C_{RB}}(v)v + \boldsymbol{M_A}\dot{v} + \boldsymbol{C_A}(v)v + \boldsymbol{D_{damp}}(v)v + \boldsymbol{g}(\eta) = \tau$$

Where $\boldsymbol{M_{RB}}$ and $\boldsymbol{M_A}$ are the rigid-body and added mass matrices, respectively; $\boldsymbol{C_{RB}}(\boldsymbol{v})$ is the rigid-body Coriolis and centripetal matrix induced by $\boldsymbol{M_{RB}}$ due to the rotation of the body frame about the NED world frame while $\boldsymbol{C_A}(\boldsymbol{v})$ is the added mass Coriolis and centripetal matrix induced by $\boldsymbol{M_{RB}}$ due to the rotation of the body frame about the NED world frame. $\boldsymbol{D_{damp}}(\boldsymbol{v})$Is the damping matrix.$\boldsymbol{g}(\boldsymbol{\eta})$ Is the restoring matrix. $\boldsymbol{\tau}$ Is the thrust matrix. M_{RB} due to the rotation of the body frame about the NED world frame and could be written as:

$$M_{RB} = \begin{bmatrix} m & 0 & 0 & 0 & mz_g & -my_g \\ 0 & m & 0 & -mz_g & 0 & mx_g \\ 0 & 0 & m & my_g & -mx_g & 0 \\ 0 & -mz_g & my_g & I_x & -I_{xy} & -I_{xz} \\ mz_g & 0 & -mx_g & -I_{yx} & I_y & -I_{yz} \\ -my_g & mx_g & 0 & -I_{zx} & -I_{zy} & I_z \end{bmatrix}$$

Moments of inertia: (kilograms * square meters)
Taken at the center of mass and aligned with the output coordinate system.

Lxx = 0.26	Lxy = 0.00	Lxz = 0.00
Lyx = 0.00	Lyy = 0.37	Lyz = 0.00
Lzx = 0.00	Lzy = 0.00	Lzz = 0.49

Where the weight and buoyancy of the ROV are shown in the table II

TABLE II
ROVS' WEIGHT AND BUOYANCY

	Weight	Buoyancy	Delta
Value (Kg)	14.6709	17.088	2.4171
X-Coordinate(mm)	254.04	254.04	0
Y-Coordinate(mm)	-43.1	-27.09	16.01
Z-Coordinate(mm)	87.45	87.45	0

The rigid-body Coriolis and centripetal matrix is induced by

$$C_{RB}(v) = \begin{bmatrix} 0 & 0 & 0 & 0 & mw & 0 \\ 0 & 0 & 0 & -mw & 0 & 0 \\ 0 & 0 & 0 & mv & -mu & 0 \\ 0 & mw & -mv & 0 & I_z r & -I_y q \\ -mw & 0 & -mu & -I_z r & 0 & I_x p \\ mv & -mu & 0 & I_y q & -I_x p & 0 \end{bmatrix}$$

For most practical applications, the off-diagonal terms of mass matrix (MA) are small compared with the diagonal ones. Since motions between DOFs are assumed to be decoupled, the off-diagonal terms of MA can be neglected. Subsequently, the added mass matrix MA can be simplified as:

$$M_A = -\begin{bmatrix} X_{\dot{u}} & 0 & 0 & 0 & 0 & 0 \\ 0 & Y_{\dot{v}} & 0 & 0 & 0 & 0 \\ 0 & 0 & Z_{\dot{w}} & 0 & 0 & 0 \\ 0 & 0 & 0 & K_{\dot{p}} & 0 & 0 \\ 0 & 0 & 0 & 0 & M_{\dot{q}} & 0 \\ 0 & 0 & 0 & 0 & 0 & N_{\dot{r}} \end{bmatrix}$$

Where are $X_{\dot{u}}$, $Y_{\dot{v}}$, $Z_{\dot{w}}$ the added mass in the x-, y- and z-axis directions due to $\dot{u}, \dot{v}, \dot{w}$ accelerations respectively, and $K_{\dot{p}}, M_{\dot{q}}, X_{\dot{r}}$ are the added inertias around the x-, y- and z-axis directions due to $\dot{p}, \dot{q}, \dot{r}$ rotational accelerations, respectively. The fluid-structure interaction (FSI) on COMSOL Multiphysics is used to simulate the oscillatory behavior of the ROV and calculate the added mass and inertia terms. The displacement, x, of the oscillating ROV is given by:

$$m_{eq}\ddot{x} + c\dot{x} + kx = 0$$

Where m_{eq} is the total mass of the ROV, c is the damping coefficient and k is the spring's stiffness. If no external harmonic excitation is applied to the ROV, the oscillation's frequency corresponds to the natural frequency,w_n of the ROV such that

$$w_n = \sqrt{\frac{k}{m_{eq}}}$$

When the ROV oscillates in a fluid, the natural frequency of the ROV is given by:

$$w_n = \sqrt{\frac{k}{m + m_a}}$$

Where m is the true mass of the ROV and ma is the added mass to the system. Thus, the added mass is

$$m_a = \frac{k}{w_n} - m = \frac{T^2 \times k}{4\pi^2} - m$$

Where T is the period of oscillation. The angular oscillation of a torsional spring-mass system is shown as:

$$w_n = \sqrt{\frac{k_t}{I_{eq}}} = \sqrt{\frac{k_t}{I + I_a}}$$

Hence,

$$I_a = \frac{T^2 \times k_t}{4\pi^2} - I_{ii}, \quad i = x, y, z$$

Using COMSOL MULTIPHYISCS program, the time step for the FSI simulations is 0.01 s and a segregated direct solver is used. The mesh deformation is controlled using the Arbitrary Lagrangian-Eulerian (ALE) algorithm to couple the fluid flow (Eulerian or spatial frame) with the solid mechanics (Lagrangian or material frame). The interaction is fully coupled; the pressure and viscous forces from the fluid are transmitted to the solid, and the displacement of the ROV wall is used as boundary conditions for the fluid flow. In the FSI model, the equations solved on COMSOL Multiphysics are the Navier- Stokes equations (the flow solver is assumed laminar), the rigid body equation of motion, and the equation coupling the solid displacement to the fluid velocity given by:

$$V_{wall} = \frac{du_{solid}}{dt}$$

For the simulation of translational and rotational oscillations, the stiffness of the spring and the mass of the ROV are chosen in a way to achieve accurate estimation of the period of oscillation and added mass. For example, choosing a spring with high stiffness increases the error in the estimation of *ma.*

TABLE III
ROVs' MOMENT OF INERTIA

Parameters	Value
Water density (ρ)	1000 Kg/m^3
ROV density (ρ_{ROV})	908 Kg/m^3
ROV mass in the FSI simulation (m)	7.81 Kg
ROV inertia in roll direction (I_{xx})	0.14 Kg.m^2
ROV inertia in pitch direction (I_{yy})	0.23 Kg.m^2
ROV inertia in yaw direction (I_{zz})	0.26 Kg.m^2
Stiffness of translational spring (K)	10000 N/m
Stiffness of rotational spring (K_t)	5000 N.m/rad
Initial excitation in translational direction	0.01 m
Initial excitation in rotational direction	0.1 rad

C. Added Mass Matrix In X-Direction

The dynamic model has been built Using COMSOL MULTIPHYISCS program. Figure 1 shows the domain size, boundaries, and the tetrahedral fine mesh used in calculations.

Then the displacement curve can be obtained as shown in fig.2.

It is shown by the curve that time period can be calculated.

Time period in surge direction = 0.275 seconds.

$$m_a = \frac{T^2 \times K}{4\pi^2} - m$$

$$m_a = \frac{0.338^2 \times 10000}{4\pi^2} - 7.81 = 21.1283 \text{ Kg}$$

$$m_a = \frac{0.275^2 \times 10000}{4\pi^2} - 7.81 = 11.346\ Kg$$

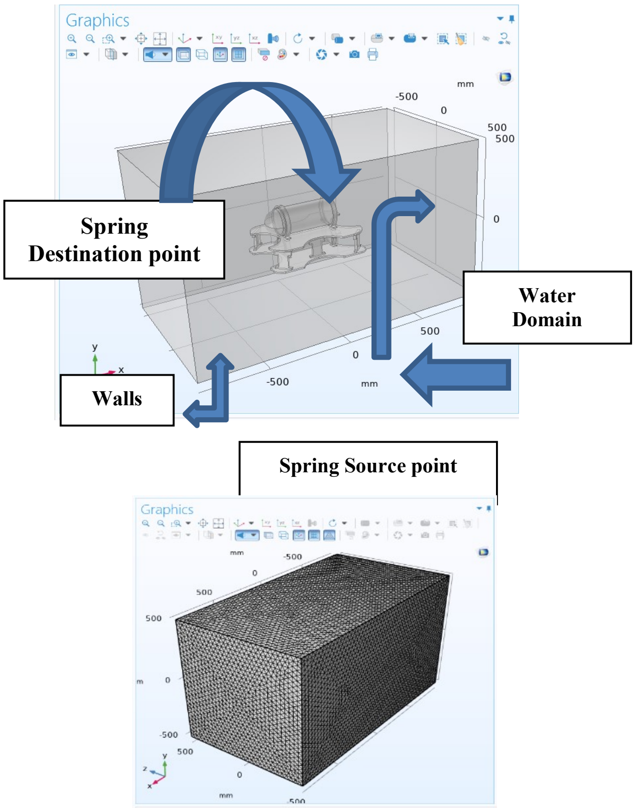

Fig. 1 Domain Boundaries and Tetrahedral mesh

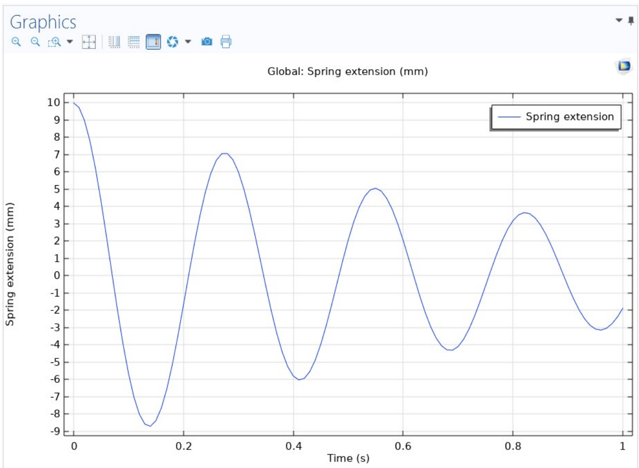

Fig. 2 Displacement curve of ROV in Surge direction due to free oscillation under water by spring system

A. Added mass parameter in z-direction (Sway)

Time period in sway direction = 0.5055 seconds, then added mass can be calculated by the equation:

$$m_a = \frac{T^2 \times K}{4\pi^2} - m$$

$$m_a = \frac{0.5055^2 \times 10000}{4\pi^2} - 7.81 = 56.9165\ Kg$$

It is noted that the added mass in heave direction is the largest value among other directions and this is because of the large force required to accelerate the water in heaving direction.

D. Added Mass Matrix In Y-Direction

In the same manner , the added mass in y-direction (heaving are determined

$$m_a = \frac{0.275^2 \times 10000}{4\pi^2} - 7.81 = 11.346\ Kg$$

E. Added Mass Matrix In Z-Direction

Time period in Z-direction (sway) = 0.338 seconds. Then added mass can be calculated in the same manner.

F. Added Inertia parameter in rotation about x axis (Rolling)

As shown in Fig. 3, Time period of the oscillation = 0.0772 seconds. The added mass moment of inertia of the ROV could be calculated as follow:

$$I_a = \frac{T^2 \times K_t}{4\pi^2} - I_{xx}$$

$$I_a = \frac{0.0772^2 \times 5000}{4\pi^2} - 0.26 = 73.19204\ Kg.m^2$$

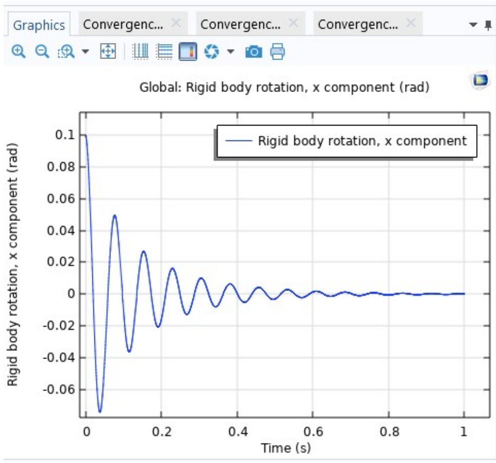

Fig. 3 ROV time oscillation

G. Added mass Coriolis and centripetal matrix

The added mass Coriolis and Centripetal matrix are written as:

$$C_A(\nu) = \begin{bmatrix} 0 & 0 & 0 & 0 & z_{\dot{w}}w & 0 \\ 0 & 0 & 0 & -z_{\dot{w}}w & 0 & -X_{\dot{u}}u \\ 0 & 0 & 0 & -Y_{\dot{v}}v & X_{\dot{u}}u & 0 \\ 0 & -z_{\dot{w}}w & Y_{\dot{v}}v & 0 & -N_{\dot{r}}r & M_{\dot{q}}q \\ z_{\dot{w}}w & 0 & -X_{\dot{u}}u & N_{\dot{r}}r & 0 & -K_{\dot{p}}p \\ -Y_{\dot{v}}v & X_{\dot{u}}u & 0 & -M_{\dot{q}}q & K_{\dot{p}}p & 0 \end{bmatrix}$$

Where u, v, w, p, q, r are linear and angular velocities respectively.

III. DAMPING MATRIX

There are four major sources causing hydrodynamic damping for a marine craft, including potential damping, wave drift damping, skin friction and damping due to vortex shedding [2] (Fossen 2011). The effects of potential damping and wave drift damping are neglected for underwater vehicles. Subsequently, the ROV damping (ν) can be approximated with a linear damping term D_L caused by skin friction and a quadratic damping term $D_{NL}(\nu)$ mainly due to vortex shedding expressed by:

$$D(\nu) = D_L(\nu) + D_{NL}(\nu)$$

The linear and quadratic terms of the damping matrix are obtained by measuring the drag force $F(u)$ at different velocities u of the ROV and calculating the coefficients of the quadratic fitting function between $F(u)$ and u. For example, for the surge direction.

$$\mathrm{F(u) = K_L u + K_q u^2}$$

Where Fu is the drag force in the surge direction. Similar equations are used for the other translational DOFs. Moreover, a quadratic equation relates the damping moment M to the angular velocity p in all rotational DOF. For example, in the roll direction.

$$\mathrm{M(p) = K_L p + K_q p^2}$$

The damping force (moment) for each translational (or rotational) velocity is obtained on ANSYS CFX by solving the Navier-stokes equations. To model the turbulence, Reynolds Averaged Navier-Stokes Equations (RANS) are solved using the k-ε model.

A. In Surge Direction

Hence, the inlet, top, bottom and sides of the domain are at a distance equal the length from the center of and the outlet is at a distance 4L downstream of the

The linear and quadratic terms are obtained by estimating a fitting function between the force (moment) and translational (rotational) velocity. In the translational direction, the computational domain is a rectangle and the dimensions of the domain are calculated such that there is no effect of the surrounding boundaries on the ROV

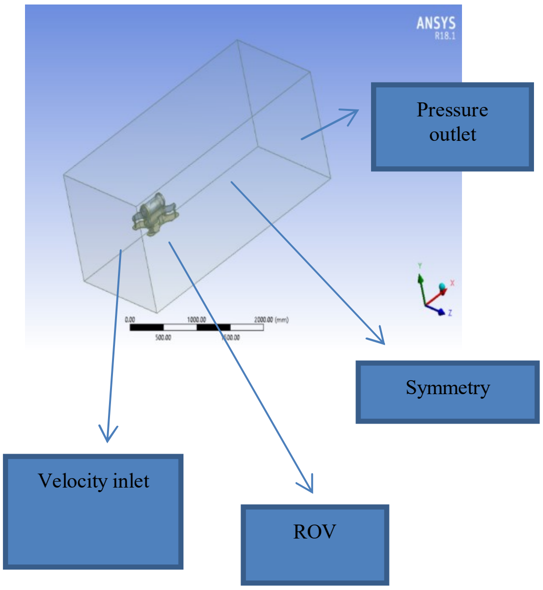

Fig. 4 Domain Size and Boundaries

The numerical calculations has been performed in the range of Froud number range Fr = 0.1-1 with 0.1 step variation.

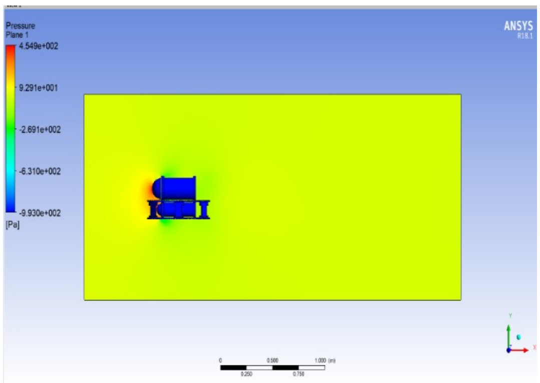

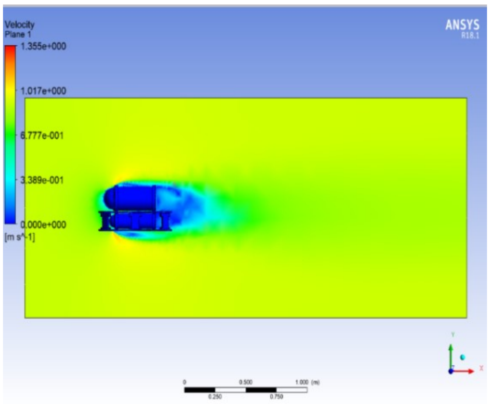

Fig. 5 Pressure variation (top) and velocity profile (down) around ROV

Figure 5 illustrate the pressure and velocity pattern around the ROV at steady velocity = 0.9 m/s in surge direction (X-Direction).

So, from fitting the curve between the resultant drag force and velocities (fig. 6), the coefficients of x^2 and x are the quadratic and linear damping coefficients respectively.

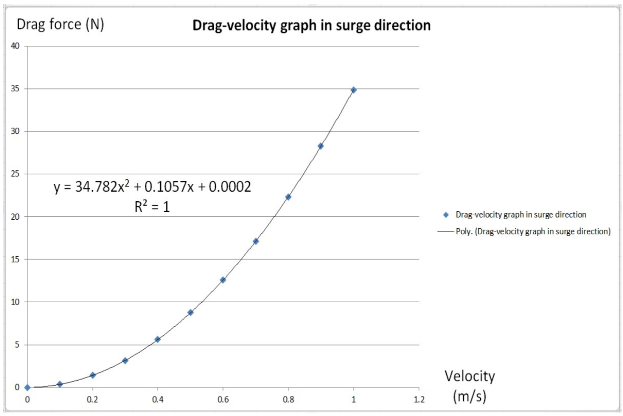

Fig. 6 Drag Force versus ROV Velocity in X-direction

In the same manner, the damping coefficients can be determined for the other degrees of freedom as presented in figure7.

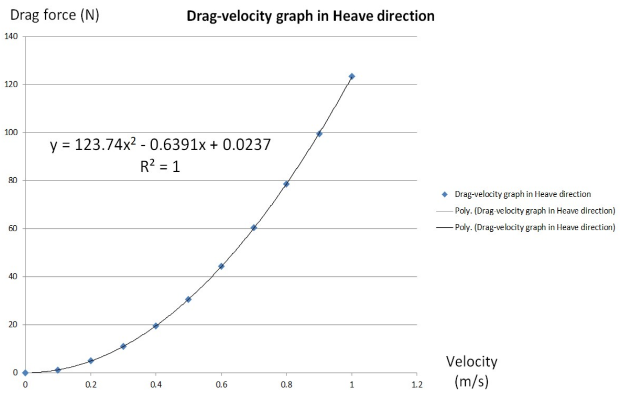

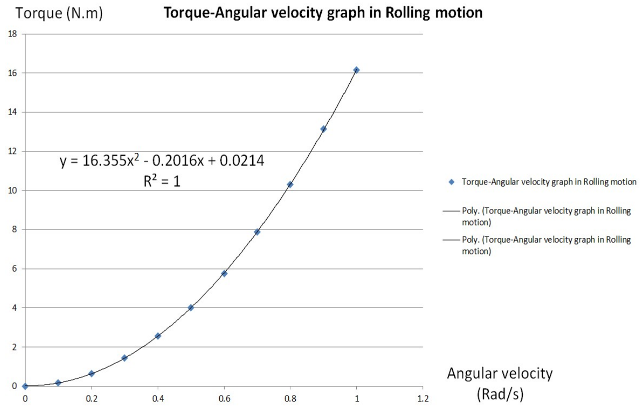

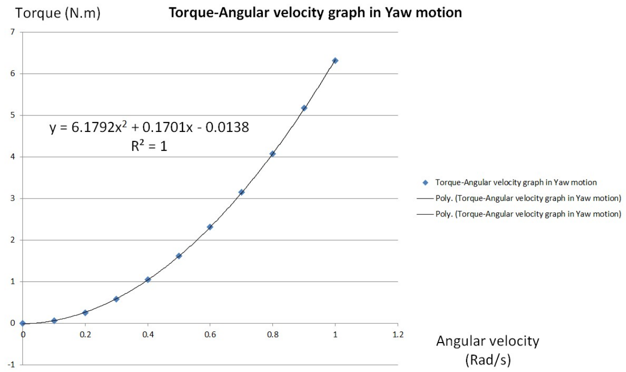

Fig. 7 Drag Force versus ROV Velocity in Heaving, Rolling, and Yaw Motions

Where R^2 Term refers to the accuracy of the equation which represents the graph points. The closer to unity, the better is the accuracy.

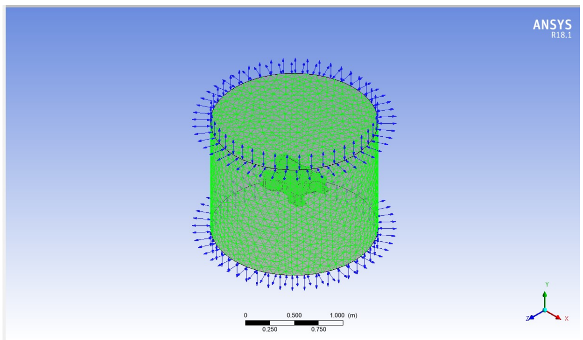

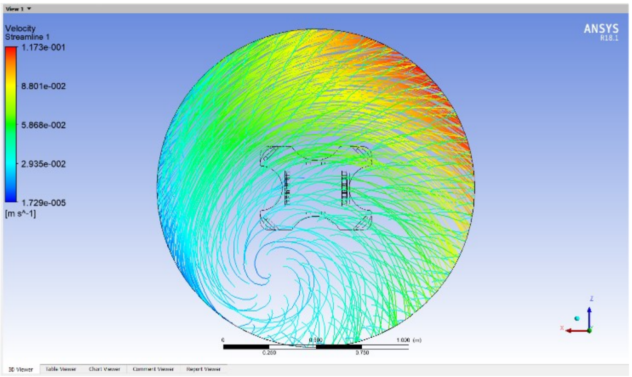

Fig. 8 Velocity profile around ROV 3D domain (top) and plan view (down) at steady angular velocity = 0.1 rad/s about Y-Axis (Yaw motion)

Simulation has been investigated by simulated the rotating domain of the ROV about Y-Axis (YAW) and the outer boundary was taken as (Opening) at steady angular velocity = 0.1 rad/s about Y-Axis (Yaw motion) (approximately 0.954 RPM) to calculate the damping torque as shown in fig. 8.

III. Restoring Matrix

The buoyancy force of ROVs is usually slightly larger than their weights to ensure that in the case of power loss the ROV resurfaces. However, we assume that the buoyancy force is equal to the weight in water for simplification, therefore, W ≈ B = m × g = 12.96 × 9.81 = 127.1376 N. The distance between the center of buoyancy and center of gravity is zb. The estimated B and zb are then used to compute the restoring matrix

$$g(\eta) = \begin{bmatrix} (W-B)\sin\theta \\ -(W-B)\cos\theta\sin\phi \\ -(W-B)\cos\theta\cos\phi \\ z_g W\cos\theta\sin\phi \\ z_g W\sin\theta \\ 0 \end{bmatrix}$$

Given W= 14.6709 Kgf, and Zg= 16.01 mm. So, the restoring matrix can be written as:

$$g(\eta) = \begin{bmatrix} 0 \\ 0 \\ 0 \\ 2.301\cos(\theta)\sin(\phi) \\ 2.301\sin(\theta) \\ 0 \end{bmatrix}$$

IV. Thrust Configuration Matrix

Given the force vector f= [Fx, Fy, Fz] and the moment arms r= [lx, ly, lz], the forces and moments in 6 DoFs can be determined by:

$$\tau = \begin{bmatrix} f \\ r \times f \end{bmatrix} = \begin{bmatrix} F_x \\ F_y \\ F_z \\ F_z l_y - F_y l_z \\ F_x l_z - F_z l_x \\ F_y l_x - F_x l_y \end{bmatrix}$$

Where T is the thrust configuration matrix and α is the thrust rotation angle vector. The moment arms of 6 thrusters relative to center of gravity (CG) are computed and listed in next table

TABLE IV
ROVs' Thrusters Moment Arm

T_i	L_{xi} (mm)	L_{yi} (mm)	L_{zi} (mm)
T_1	292.67	-26.55	217.25
T_2	292.67	-26.55	-217.25
T_3	-269.75	-26.55	-235.42
T_4	-269.75	-26.55	235.42
T_5	2.5	-39.29	188.25
T_6	2.5	-39.29	-188.25

The rotation angles for horizontal thrusters of T_1 to T_4 are $\pi/4$, $-\pi/4$, $-3\pi/4$ and $3\pi/4$, respectively and thruster T_5 and T_6 are vertical thrusters without horizontal rotations. Subsequently, the forces and moments produced by thruster T_1 can be computed by:

$$\tau = \begin{bmatrix} F_{x1} \\ F_{y1} \\ F_{z1} \\ F_{z1} l_{y1} - F_{y1} l_{z1} \\ F_{x1} l_{z1} - F_{z1} l_{x1} \\ F_{y1} l_{x1} - F_{x1} l_{y1} \end{bmatrix} = \begin{bmatrix} F1 \times \cos(45) \\ 0 \\ -F1 \times \sin(45) \\ F1\sin(45) \times 26.55 \\ -F1\cos(45) \times 217.25 - F1\sin(45) \times 292.67 \\ 0 - F1\cos(45) \times -26.55 \end{bmatrix} = \begin{bmatrix} -0.707 \\ 0 \\ 0.707 \\ 18.77 \\ -360.56 \\ 18.77 \end{bmatrix} F_1$$

Hence,

$$t_1 = \begin{bmatrix} -0.707 \\ 0 \\ 0.707 \\ -18.77 \\ -360.56 \\ -18.77 \end{bmatrix}$$

By following the same procedure, the forces and moments produced by total 6 thrusters are found to be:

$$\tau=(\alpha)F=\begin{bmatrix} -0.707 & 0.707 & -0.707 & -0.707 & 0 & 0 \\ 0 & 0 & 0 & 0 & 1 & 1 \\ 0.707 & 0.707 & 0.707 & -0.707 & 0 & 0 \\ -0.018 & -0.018 & -0.018 & 0.018 & -0.188 & -0.188 \\ -0.36 & -0.36 & 0.36 & -0.36 & 0 & 0 \\ -0.018 & 0.018 & -0.018 & -0.018 & 2.5 & 2.5 \end{bmatrix} \times \begin{bmatrix} F_1 \\ F_2 \\ F_3 \\ F_4 \\ F_5 \\ F_6 \end{bmatrix}$$

Then, the thrust configuration matrix can be found.

$$T=\begin{bmatrix} -0.707 & 0.707 & -0.707 & -0.707 & 0 & 0 \\ 0 & 0 & 0 & 0 & 1 & 1 \\ 0.707 & 0.707 & 0.707 & -0.707 & 0 & 0 \\ -0.018 & -0.018 & -0.018 & 0.018 & -0.188 & -0.188 \\ -0.36 & -0.36 & 0.36 & -0.36 & 0 & 0 \\ -0.018 & 0.018 & -0.018 & -0.018 & 2.5 & 2.5 \end{bmatrix}$$

So by this matrix, we can control the ROV in all degrees of freedom. We can consider the rows as type of degree of freedom and the columns as the thruster number.

.

IV. Conclusion

After building the ROV and designing it on different software programs, it must be tested by simulation software. The ROV was designed on Solidworks and its material was chosen as Polypropylene film. The ROV stability was tested and calculated. The GZ curve was calculated. 6 Thrusters were put in the design.

The ROV simulation under the water was made by using Ansys CFD. The drag of motion was calculated. In this paper, The Dynamic model of The ROV was determined in five degrees of freedom (because The pitch rotation can be neglected due to thruster configuration). Every component in the equation of motion in all degrees of freedom were calculated and estimated as a preliminary design. The added mass was estimated using COMSOL MULTIPHYSICS

References

[1] Fossen, Thor Inge and Tor Arne Johansen. “A Survey of Control Allocation Methods for Ships and Underwater Vehicles.” *2006 14th Mediterranean Conference on Control and Automation* (2006): 1-6.

[2] Fossen, T.I. (2011) Handbook of Marine Craft Hydrodynamics and Motion Control. John Wiley & Sons, Inc., Chichester, UK. https://doi.org/10.1002/9781119994138

[3] S. Ziani-cherif, G. Lebret,On the Identification of the Nonlinear Dynamic Model of an Underwater R.O.V.(1),IFAC Proceedings Volumes,Volume 30, Issue 11,1997,Pages 651-656,ISSN 1474-6670,https://doi.org/10.1016/S1474-6670(17)42919-3.

[4] M. Nomoto and M. Hattori, "A deep ROV "DOLPHIN 3K": Design and performance analysis," in *IEEE Journal of Oceanic Engineering*, vol. 11, no. 3, pp. 373-391, July 1986, doi: 10.1109/JOE.1986.1145188

[5] Goodman, Leo A. “On the Exact Variance of Products.” *Journal of the American Statistical Association*, vol. 55, no. 292, 1960, pp. 708–13. *JSTOR*, https://doi.org/10.2307/2281592. Accessed 2 May 2023

[6] A. T. Morrison and D. R. Yoerger, "Determination of the hydrodynamic parameters of an underwater vehicle during small scale, nonuniform, 1-dimensional translation," *Proceedings of OCEANS '93*, Victoria, BC, Canada, 1993, pp. II277-II282 vol.2, doi: 10.1109/OCEANS.1993.326105.

[7] Fossen, Thor & Sagatun, Svein. (1991). Adaptive control of nonlinear underwater robotic systems. Modeling, Identification and Control: A Norwegian Research Bulletin. 12. 95-105. 10.4173/mic.1991.2.4.

[8] Egeland, Olav & Gravdahl, Jan. (2002). Modeling and Simulation for Automatic Control.

[9] S.P. Berge & T.I. Fossen, "On the Properties of the Nonlinear Ship Equations of Motion," Mathematical and Computer Modelling of Dynamical Systems, Taylor & Francis Journals, vol. 6(4), pages 365-381, December 2000.

[10] M. Badawy, A. A. Omer, " Stress and dynamic analysis of simple remotely operated underwater vehicle ", AMME Conference, 29-31 May, 2012

[11] Chu-Jou Wu, " 6-DoF Modelling and Control of a Remotely Operated Vehicle", Flinders University, College of Science and Engineering, July, 2018.